Heliyon 8 (2022) e09955

Contents lists available at ScienceDirect

Heliyon

journal homepage: www.cell.com/heliyon

Research article

The intestinal absorption mechanism of chicoric acid and its bioavailability improvement with chitosan

Geng Nan Wang [a], Yi Peng Li [a], Si Kun Yuan [b], Hu Zhang [a], Juan Ren [a], Xin Ren [a], Ju Xiang Liu [a,*]

[a] College of Veterinary Medicine, Hebei Agricultural University, Baoding, Hebei, 071000, PR China
[b] Baoding Institute for Food and Drug Control, Baoding, Hebei, 071000, PR China

ARTICLE INFO

Keywords:
Chicoric acid
Caco-2
Chitosan
Intestinal transport
Pharmacokinetics

ABSTRACT

Chicoric acid (CA), an active phenolic acid of *Echinacea purpurea (Linn.) Moench*, has been demonstrated to exhibit antioxidative, antiviral and immunological activities. A prior study showed that CA is a water-soluble compound with low bioavailability. The current study was performed to study the intestinal absorption mechanism of CA and improve its bioavailability using natural biodegradable chitosan. A Caco-2 monolayer cell model was established to characterise the mechanisms involved in the intestinal absorption of CA. The bioavailability improvement of CA was studied in Sprague–Dawley rats after oral (20 mg/kg) administration of 0.5% chitosan. In vitro, the results showed that the absorption transport of CA was fairly poor, with Papp values of 8.2×10^{-8} to 2.1×10^{-7} cm/s in the absorption direction and 1.5×10^{-7} to 2.6×10^{-7} cm/s in the secretory direction. The permeability was increased by EDTA and chitosan in both directions. Moreover, the transport through the intestinal monolayer was H^+ dependent, and P-glycoprotein and OATP2B1 transporters were involved in the intestinal transport of CA. In vivo, the absorption of CA was increased and accelerated with chitosan in rats because the bioavailability was 1.74-fold that of the prototype drug. The above mentioned results indicated that CA was a poor absorption drug and that paracellular and carrier-mediated trancellular transport both participated in its transport route. Chitosan is an excellent absorption enhancer for CA. The transport characteristics uncovered in this study lay the groundwork for further studies directed toward the development and utilisation of its new formulations.

1. Introduction

Chicoric acid (CA), a caffeic acid derivative (Figure 1), is an active component of *Echinacea purpurea (Linn.) Moench* has been widely used as a dietary supplement and an immunopotentiator agent worldwide for its strong potent bioactivities [1, 2, 3, 4]. According to a previous study, CA possesses protective effects on the lung, liver and kidney [5], while CA also exhibits strengthened antioxidant and antiviral (EV-A71, HSV, HIV and Ebola) activities [6, 7, 8, 9, 10, 11]. Recent studies have shown that CA could become an effective drug for gout [12] and type II diabetes [13]. Although more studies have been performed on CA in recent years, they have mainly focused on its pharmacological activities and few reports on its pharmacokinetics in vivo. A previous study by our team reported that the absolute bioavailability of CA in rats is quite low, only approximately 2.0%, and the excretion of the prototype in urine accounts for 15.3% of the dosage [14]. Therefore, it is necessary to investigate the intestinal absorption mechanism of CA to improve its bioavailability.

At present, oral routes are preferred for the administration of therapeutic compounds; however, the poor bioavailability of new drug candidates is a barrier to their development in oral form. Intestinal permeation enhancers are one of the most widely tested strategies to improve oral delivery. However, few absorption enhancers are presently used clinically due to the difficulty of developing enhancers with high specificity and low toxicity. For example, polysorbate and polyoxyethylene could lead to the dissolution of cell membrane components in the process of mucosal permeability promotion [15]; sodium dodecyl sulfate and polyoxyethylene could cause irreversible damage to intestinal epithelial cells [16]; sodium laurate could cause apoptosis [17]; and bile salt at high concentrations would cause cytotoxicity [18]. Chitosan, a polysaccharide derived from naturally occurring chitin, has been exhibited biological compatibility, biodegradability, antimicrobial and antioxidant activity [19]. Due to its safety and effectiveness, it has been used in a large number of fields, such as food preservation, the pharmaceutical industry and feed additives [20, 21, 22]. Additionally, chitosan has been proven to be a paracellular opener. It can be used as safe

* Corresponding author.
E-mail address: liujuxiang0315@sina.com (J.X. Liu).

https://doi.org/10.1016/j.heliyon.2022.e09955
Received 31 January 2022; Received in revised form 18 April 2022; Accepted 11 July 2022

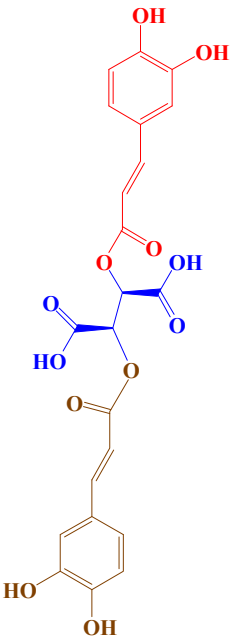

Figure 1. Chemical structures of chicoric acid (MW 474.37112 Da).

and effective intestinal absorption enhancers due to their mucosal adhesion, reversible opening of tight junctions and positive charge [23, 24]. The mechanism of tight junction integrity reduction is related to the changes in transmembrane CLDN4 protein induced by chitosan which can be used as a permeation enhancer for the absorption of hydrophilic drugs that have a paracellular transport mechanism [25].

It is well known that intestinal transporters play an important role in the intestinal absorption of drugs nowadays. Efflux transporters such as ABCB1 (P-gp, MDR1) and ABCG2 (BCRP) may limit the oral bioavailability of drugs while several solute carriers including ASBT (SLC10A2) and PEPT1 (SLC15A1) contribute to the uptake of their substrates into the intestinal epithelia [26]. P-gp is an efflux protein regulated by a multidrug resistance gene (MDR1). It is highly expressed in the Caco-2 cell line, and is mainly distributed on the AP side of the Caco-2 monolayer and largely limits the bioavailability of some natural drugs [27, 28]. The organic anion transporting polypeptide 2B1 (OATP2B1) was one of the first cloned members of the SLCO family. OATP2B1 has been recognized as a transporter of emerging clinical importance, as its intestinal expression involved in oral drug absorption of its substrate lead to drug-drug interaction [29]. Recent studies have shown that the absence of OATP2B1 could reduce the absorption of fluvastatin by 2- to 3-fold [30].

As a result, the purpose of the current study was to elucidate the intestinal transport mechanism, improve the bioavailability of CA and serve as a theoretical basis for the development of its new formulations.

2. Materials and methods

2.1. Materials

Chicoric acid (purity ≥98%) was purchased from Mansite Biological Technology Co., Ltd. (Chengdu, China). The Caco-2 cell line was obtained from National Experimental Cell Resource Sharing Platform (Peking, China). HBSS, DMEM, FBS and other cell culture reagents were all obtained from Gibco, Thermo Fisher Scientific. Heparin sodium injection (6250 IU/mL) was purchased from Tianjin Biochem Pharmaceutical Co. Ltd. (Tinjin, China). Chromatographic grade acetonitrile and methanol were obtained from EMD Millipore Corporation (Billerica MA, USA). Analytical grade hydrochloric acid, phosphoric acid and other chemicals were obtained from Tianjin Concord Chemical Reagent Company (Tianjin, China). Ultrapure water of Milli-Q grade was used throughout the study.

2.2. Cell culture

The Caco-2 cell line, which was incubated at 37 °C with 5% CO_2, was cultured in 75 mL flasks with Dulbecco's modified Eagle's medium (DMEM) containing 10% foetal bovine serum, 1% nonessential amino acids, 1% L-glutamine, 100 IU/mL penicillin and 100 IU/mL streptomycin. The medium was changed every 2 days. When the cells grew to 80% confluence in the flasks, they were cultured with the trypsin enzyme digestion technique and passaged in vitro. The cells were used between passages 31 and 35.

For the Transwell experiment, Caco-2 cells were seeded on 6-well Transwell plates coated with rat tail collagen at a density of 3×10^5 cells/well (6×10^4 cells/cm^2). A 1.5 mL culture medium was added to the apical (A) of each well and 2.6 mL to the basolateral (B). The culture medium was changed every other day. After 21 days of culture, the drug Transwell experiment was carried out after the cells were completely differentiated and formed a dense monolayer in each well with a TEER value >900 Ω cm^2 [31].

2.3. Permeability coefficient calculation

The cell monolayers were washed twice with HBSS and equilibrated for 20 min at 37 °C before the permeability assay of CA. The standard solution of CA (100, 200, 500 μM) prepared by HBSS was loaded on the A or B side for the apical to basolateral (A – B) and basolateral to apical (B – A) direction studies, respectively. Sample aliquots of 200 μL were collected from the receiver compartment at 15, 30, 45, 60, 90, 120, and 180 min and replaced by an equal volume of blank HBSS. The samples were analysed by UPLC as detailed in 2.9. The apparent permeability coefficients (P_{app}) and efflux ratio were calculated by the following formulas:

$$P_{app} = (dC/dt)\ (V/AC_0)$$

$$\text{Efflux ratio} = P_{app}\ (B - A)/P_{app}\ (A - B)$$

where:

dC/dt: Change in chicoric acid concentration in the receiver with time.

C_0: Initial concentration in the donor chamber.

A: Surface area of the cell monolayer (4.52 cm^2 for six-well plate).

V: Volume of receiver chamber (2.6 mL for the A – B direction, 1.5 mL for the B – A direction).

2.4. Cell viability study

Cell viabilities for different drugs were measured by MTT assay. Caco-2 cells were seeded on 96-well plates at a density of 5×10^4 cells/well. After 24 h of incubation, various concentrations of drugs (CA, chitosan) prepared by HBSS replaced the culture medium. After 24 h of exposure, 10 μL of 0.5% MTT solution was added to each well and incubated for 4 h. Then, the supernatant was drained and replaced with 150 μL DMSO. Finally, the absorbance was measured at 490 nm by a microplate reader.

2.5. Paracellular pathway study

The intercellular opener EDTA and chitosan were used to evaluate the participation of the paracellular pathway of CA. For EDTA, the cell monolayer was incubated with 5 mM EDTA in D-HBSS (free of Ca^{2+} and Mg^{2+}) for 5 min. Then, the standards of CA (500 μM) prepared with 50% HBSS and 50% D-HBSS were loaded into the apical and basolateral compartments. The receiver medium was collected at 15, 30, 45, 60, 90, 120, and 180 min. For chitosan, 0.05% chitosan solution prepared by HBSS with pH 6.3 was added to the apical compartment, and the

standards of CA (500 μM) were loaded to the apical and basolateral compartments. The receiver medium was collected at the same time points above. The TEER values were evaluated at the beginning of the experiment and 24 h later. The Papp values for both directions were calculated after determining the concentration of CA.

2.6. Effect of pH on transport

The effect of pH on the transport of CA (500 μM) was evaluated at pH 6.3 compared to pH 7.4. The medium of pH 6.3 was prepared by HBSS adjusted pH to 6.3 with 1 *M hydrochloric* acid, whereas the pH of HBSS was 7.4. The Papp values for both directions were calculated after determining the concentration of CA.

2.7. Effect of P-glycoprotein and OATP2B1 transporter

GF120918 (a potent, specific Pgp inhibitor) [32] and 6 μM baicalin (an OATP2B1 inhibitor) [33] were used at 2 μM to confirm that the compound was a P-glycoprotein (Pgp) and OATP2B1 substrate. Both transporter inhibitors were loaded to the apical compartment and used for the transport study of CA from the A–B or B–A direction as described above.

2.8. Statistical analysis

All the cell treatments were performed at least in triplicate and expressed as the mean ± SD. A t test was used for the differences between groups. Statistical significance was accepted at $p < 0.05$.

2.9. Determination of CA

The Waters Acquity UPLC H-Class system (Waters, Milford, MA, USA) included a quaternary solvent manager, an autosampler set at 4 °C and a Waters Acquity UPLC Shield RP18 column (100 × 2.1 mm, 1.7 μm, Waters, Milford, MA, USA). The chromatographic separation was performed on isocratic elution with mobile phases of acetonitrile (A) and 0.1% phosphoric acid (B). Solvent A was 22% (v/v) at the beginning, linearly increased to 42% over 1 min, and then returned to 22% by 2 min at a flow rate of 0.3 ml/min. The detection was performed by a photodiode array detector at 327 nm.

2.10. Method validation

2.10.1. Calibration standards and QC samples

The standard stock solution of CA (1 mg/mL) and chlorogenic acid (1 mg/mL) was prepared in methanol/0.1% phosphoric acid (1:1, v/v) and stored at -20 °C for less than one week. A series of working standard solutions of CA at different concentrations (500.0–20000.0 ng/mL) was prepared by diluting the stock solution. Calibration standards were prepared by spiking 10 μL of the appropriate CA working solutions into 100 μL of blank plasma to yield a series of standard solutions of 50.0, 100.0, 200.0, 500.0, 1,000.0, and 2,000.0 ng/mL. According to the method above, the quality control (QC) samples were prepared for three different levels, which represented low, middle and high concentrations of CA at 100, 500.0, 2000.0 ng/mL in plasma.

2.10.2. Sample preparation

A 100 μL aliquot of plasma was sequentially added to 20 μL of 10 μg/mL chlorogenic acid as an internal standard, 50 μL of 1 M HCl and 1 mL of ethyl acetate to sonicate the extract and vortexed for 2 min equally. This mixture was centrifuged at 10,000 rpm for 3 min, and the supernatant was transferred into a 2 mL centrifuge tube and then concentrated to dryness under nitrogen. The analytes were dissolved in 100 μL of methanol/0.1% phosphoric acid (1:1, v/v).

2.10.3. Linearity and sensitivity

For plasma, the calibration curves of CA covered the concentration range of 50.0–2000.0 ng/mL. Qualitative analysis was performed by plotting the respective peak area versus the concentrations. The limit of detection (LOD) and the limit of quantification (LOQ) were defined as signal-to-noise ratios of 3 and 10, respectively. Moreover, the relative standard (RSD) should be lower than 20%, and the accuracy should be between 80 and 120% for the LOQ.

2.10.4. Precision, accuracy and stability

The precision (RSD) and accuracy (detected concentration/nominal concentration) were estimated by QC samples ($n = 5$) at three levels. Within-run and between-run assessments were determined by one day and three continuous days of QC samples. For stability of CA in prepared samples, the three levels of QC samples ($n = 5$) were reanalysed at 4 °C for 24 h in the autosampler.

2.11. Pharmacokinetic study

2.11.1. Animals

The animal experiment was approved by the Animal Ethics Committee at Hebei Agricultural University. Male Sprague – Dawley rats (200 ± 20 g, 6 weeks, $n = 5$) were used and supplied by SPF Biotechnology Company (Beijing, China). Under anaesthesia with an intramuscular dose of Zoletil®50 (tiletamine hydrochloride and zalazepam hydrochloride for injection, Virbac S.A., France) at 50 mg/kg (0.2 mL) to the lateral thigh muscle, light surgery was performed. The right jugular vein was cannulated with a polyethylene catheter (0.50-mm ID, 1.00-mm OD, Portex Limited, Hythe, Kent, England). After surgery, the rats were placed individually in cages and allowed to recover for at least 12 h. The rats were fasted overnight with free access to water prior to drug administration.

2.11.2. Dosing and sampling

Before each experiment, CA was dissolved in water and 0.5% chitosan solution. The solution was given to rats orally by gavage at a single oral dose (20 mg/kg). Rat ($n = 5$) blood samples (300 μL) at appropriate intervals after dosing were collected from the catheter into a heparinized centrifuge tube at 10, 20, 60, 120, 180, 240, 300, 360, 480, 720, and 1440 min, which was immediately centrifuged at 8,000 rpm for 3 min for separation of plasma. After each blood collection, 0.3 mL of normal saline containing 20 units of heparin was injected into the catheter to flush the catheter and prevent coagulation.

2.11.3. Pharmacokinetic data analysis

Pharmacokinetic parameters were estimated by plasma concentration versus time profiles using Phoenix WinNonlin software. The non-compartmental model was employed to calculate the following parameters: terminal elimination half-life ($t_{1/2,\lambda z}$), area under the plasma concentration versus time curve from zero to last sampling time ($AUC_{0\text{-}t}$) and infinity ($AUC_{0\text{-}\infty}$), total body clearance (CL) and volume of distribution ($V_{d,\lambda z}$). The peak plasma concentration (C_{max}) and the time to reach C_{max} (T_{max}) were read directly from observed individual plasma concentration-time data. Relative bioavailability (F) was calculated by the $AUC_{0\text{-}\infty}$ of CA with chitosan to that without chitosan at an equivalent dose for gavage administration.

3. Results and discussion

3.1. Cytotoxic study

The cytotoxic effects of CA and chitosan were determined by MTT assay, and the results are shown in Figure 2. The cell viability was more than 90% at concentrations ranging from 100 – 800 μM for CA and 0.01%–0.08% (100–800 μg/mL) for chitosan. Therefore, concentrations of 100, 200, and 500 μM for CA and 0.05% for chitosan were chosen for the permeability study.

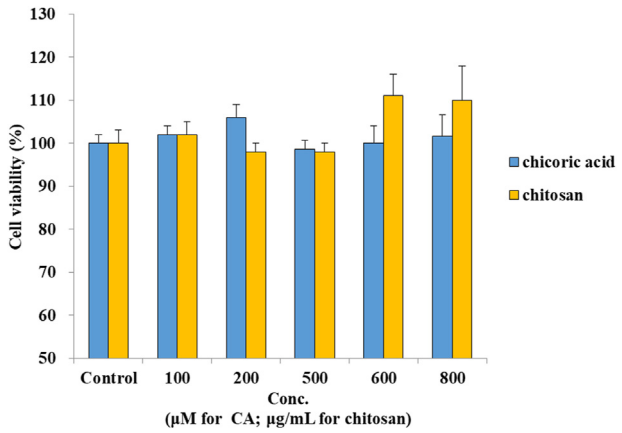

Figure 2. Effects of CA and chitosan on cytotoxicity in Caco-2 cells. All the data were expressed as % (mean ± SD, n = 5).

3.2. Permeability coefficient calculation

The results obtained after exposure of the well-developed Caco-2 cell model to CA over 180 min are shown in Figure 3. In the A to B direction, the Papp values were (2.1 ± 0.5) $\times 10^{-7}$, (8.2 ± 1.9) $\times 10^{-8}$, and (10.5 ± 1.5) $\times 10^{-8}$ cm/s for concentrations of 100, 200, and 500 μM, respectively, whereas the values were greater in the BL to AP direction, (2.6 ± 0.3) $\times 10^{-7}$, (1.5 ± 0.3) $\times 10^{-7}$, and (1.6 ± 0.1) $\times 10^{-7}$ cm/s, respectively). The efflux ratio was greater than unity, 1.2, 1.8, and 1.5 for low to high concentrations, respectively.

In the literature, a value of Papp below 1 $\times 10^{-6}$ cm/s indicates the malabsorption of the drug (0–20%), a value of Papp between 1 and 10 $\times 10^{-6}$ cm/s indicates moderate absorption (20–70%), and a value of Papp above 10 $\times 10^{-6}$ cm/s suggests high absorption (70–100%) [34]. Comparing the results obtained in the present work for CA, the Papp values at the three concentrations were all below 1 $\times 10^{-6}$ cm/s, indicating poor absorption in vivo. This fact corresponds to the results obtained in the previous work of our team in vivo, as the bioavailability of CA was only 2.0% in rats [14]. To further understand the transport mechanism of CA across the Caco-2 monolayer, two-way [apical to basolateral (A – B) and basolateral to apical (B – A)] permeation experiments were performed, and the efflux ratio was calculated. A minor existence of active transport has been investigated, where the ratio of basolateral to apical (B – A) permeability versus apical to basolateral (A – B) permeability is compared with the values of 1.5 and 2.0. If Papp (B – A)/Papp (A – B) is greater than 2.0, the active efflux or uptake mechanisms are definitely taken in charge. If an efflux ratio of 1.5–2.0, a transport experiment with increasing concentrations should be performed to investigate if the flux rate is concentration-dependent and Pgp inhibitor will be used to confirm the compound was a Pgp substrate. Otherwise, no significant differences between the Papp values in the two directions indicate that the absorption mechanism may simply be passive diffusion [32, 35]. In the present work, the Papp values tended to decrease with increasing concentrations. When the concentration of CA was higher than 200 μM, the efflux ratios were all higher than 1.5 (1.8 for 200 μM and 1.5 for 500 μM), which were between 1.5 and 2.0, indicating that the flux rate is concentration-dependent and that transcellular pathway transport exists.

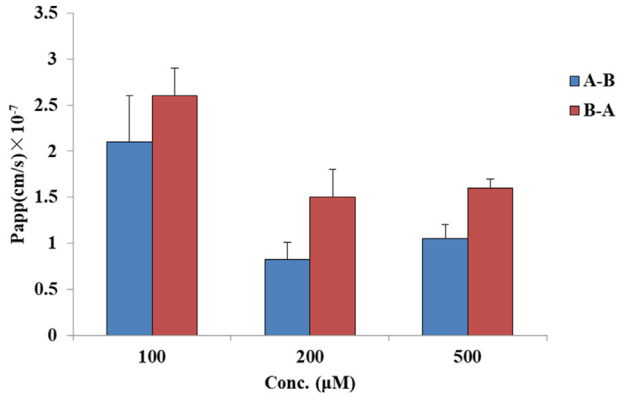

Figure 3. Permeability evaluations of CA at different concentrations. Apical – Basolateral (A–B) and Basolateral – Apical (B–A). All the data are expressed as cm/s (mean ± SD, n = 3). Significant differences were accepted at $p < 0.05$ (*).

3.3. Effect of EDTA on transport

To explore the paracellular transport of CA, the cell monolayer was preincubated with EDTA, which is known as a modulator of paracellular permeability, by opening tight junctions [36, 37]. The intercellular opener EDTA markedly altered intercellular junctions. After 5 min of incubation with EDTA solution, the TEER values decreased by 80%, which indicated that the cell junction was obviously opened. The Papp values of CA in the A – B and B – A directions following EDTA incubation and before this treatment are shown in Figure 4. The Papp values of CA with EDTA treatment were (4.5 ± 0.4) $\times 10^{-6}$ and (2.5 ± 0.2) $\times 10^{-5}$ cm/s for the A – B and B – A directions, respectively, approximately 55-fold in the A – B direction and 167-fold in the B – A direction compared to the treatment without EDTA.

There are two pathways of drug transport through the intestinal epithelium: paracellular and transcellular transport. Paracellular transport involves only a passive diffusion mechanism, whereas transcellular transport can be mediated by passive, facilitated or active processes [38]. The present study exhibited a significant increase in the permeability of CA with EDTA in both directions. This indicates that paracellular transport plays an important role in the absorption of CA across the intestinal epithelium. This could also explain why the values of Papp of CA are low. Less than 0.1% of the total surface area of the intestinal epithelium is paracellular, and drug absorption is limited by tight junctions between epithelial cells [39]. Generally, hydrophilic drugs have poor bioavailability due to their paracellular transport.

3.4. Effect of chitosan and pH on transport

To increase the absorption of CA, a hydrophilic macromolecule, the permeation enhancer chitosan which could decrease tight junction integrity in Caco-2 cells, has been evaluated. The pH 6.3 HBSS was chosen for this experiment because of the poor solution of chitosan in neutral and alkaline

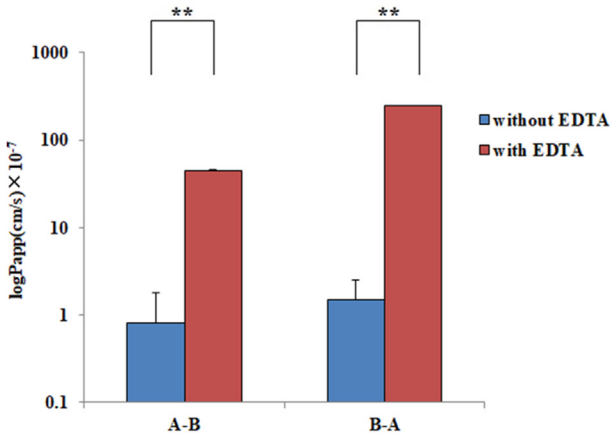

Figure 4. Permeability evaluations of CA with EDTA treatment and without EDTA in the A – B and B – A directions. All the data were from three replications and expressed as log (cm/s) (mean ± SD, n = 3). Significant differences with respect to the control (without EDTA) at $p < 0.01$ (* *).

conditions and significant toxicity to cells when the pH values were lower than 6.3. The Papp values of CA in the A – B and B – A directions with chitosan treatment in Caco-2 monolayers were (2.1 ± 0.1) $\times 10^{-7}$ and (2.3 ± 0.3) $\times 10^{-7}$ cm/s, respectively. For the pH 6.3 condition, the Papp values were (6.7 ± 1.2) $\times 10^{-8}$ and (2.5 ± 0.3) $\times 10^{-7}$ cm/s in both directions above. As Figure 5 shows, in the A – B direction, the permeability with chitosan was approximately 3-fold that at pH 6.3 without chitosan. Furthermore, corresponding to the pH 7.4 (HBSS) condition, H^+ would significantly improve the transport in the B – A direction of CA.

Several hydrophilic drugs cannot pass through the lipid bilayer of the cell membrane, so the paracellular pathway becomes the main route of their absorption [40]. In pH6.3 environment, chitosan significantly increased the transport in both directions, resulting in an efflux ratio value approaching 1.0. These results showed that chitosan could promote the absorption of CA in vitro, also suggesting the existence of a paracellular pathway transport mechanism. Additionally, compared with pH 7.4, H^+ significantly improved the transport in the B – A direction, and there was no obvious difference in the A – B direction at pH 6.3. Most organic anion-transporting polypeptides (OATP) are pH-dependent [41, 42]. For instance, the established OATP2B1 substrates demonstrated markedly higher transport from the B – A direction than in the opposite direction across Caco-2 cell monolayers at pH 5.0 [43]. As the pH in the small intestinal microenvironment is approximately pH 6.3 [44], the physiological transport activity of OATP2B1 could be higher than pH 7.4. A recent report showed that OATP2B1 in the jejunum was expressed dominantly on the basolateral side [45]. The present results indicate that CA was H^+-dependent because the Papp value in the B – A direction was significantly increasing and approximately 3-fold that in the A – B direction at pH 6.3, which is consistent with the character of OATP2B1.

3.5. Effect of P-glycoprotein and OATP2B1 transporters

To evaluate the active transport mechanism of CA on the essential p-glycoprotein and OATP2B1 transporters, Papp values were evaluated as described in Figure 6. After P-glycoprotein (Pgp) inhibitor (GF120918) treatment, the average Papp value of CA in the A – B direction was significantly increased 1.75-fold from (1.1 ± 0.2) $\times 10^{-7}$ to (1.8 ± 0.3) $\times 10^{-7}$ cm/s and decreased 62% from (1.6 ± 0.1) $\times 10^{-7}$ to (0.6 ± 0.2) $\times 10^{-7}$ cm/s in the B – A direction. After treatment with an OATP2B1 inhibitor (baicalin), the average Papp value decreased 63% from (1.6 ± 0.1) $\times 10^{-7}$ to (0.6 ± 0.1) $\times 10^{-7}$ cm/s in the B – A direction, but there was no significant change in the A – B direction. The results indicate that CA is an essential substrate of p-glycoprotein and OATP2B1 transporters.

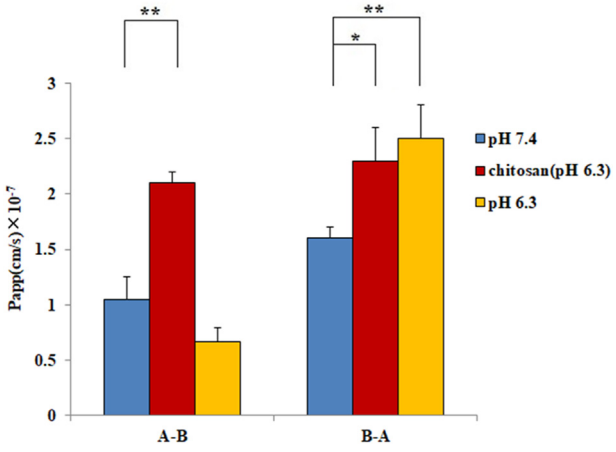

Figure 5. Permeability evaluations of CA at pH 7.4 (HBSS), pH 6.3, and chitosan treatment in the A – B and B – A directions. All the data were from three replications and expressed as cm/s (mean ± SD, n = 3). Significant differences with respect to the control (HBSS) at $p < 0.05$ (*) and $p < 0.01$ (* *).

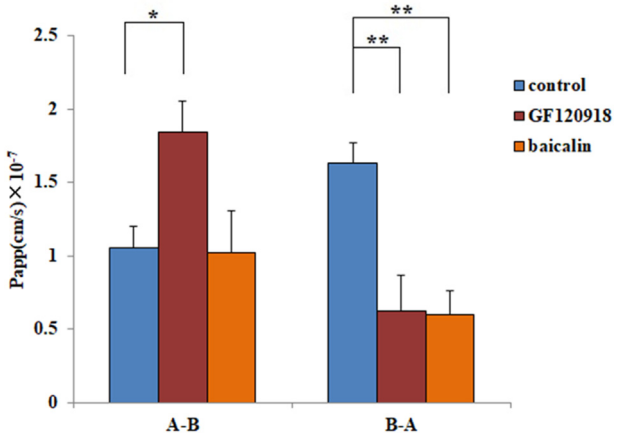

Figure 6. Permeability evaluations of CA with GF120918 (Pgp inhibitor) and baicalin in the A – B and B – A directions. All the data were from three replications and expressed as cm/s (mean ± SD, n = 3). Significant differences with respect to the control (HBSS) at $p < 0.05$ (*) and $p < 0.01$ (* *).

P-gp excretes intracellular drugs as a substrate, which makes the secretion rate of the B – A side faster than that of A – B. GF120918 is a specific Pgp inhibitor. After treatment with 2 μM GF120918 [32], the Papp value significantly reduced the transport rate of CA in the B – A direction and increased it in the A – B direction. The results suggest that CA is a potential substrate of Pgp. A previous study showed that baicalin effectively reduced the influx of substrates of OATP2B1 with an IC50 value of 5.6 ± 3.2 μM [33]. As a result, 6 μM baicalin was used as an OAPT2B1 inhibitor, and the Papp value was significantly reduced from B to A and did not change from A to B under its treatment. The results indicate that OATP2B1 might participate in the intestinal absorption of CA, but this effect is minor compared with the results of EDTA treatment.

3.6. Method validation

The calibration curve was y = 0.0011x – 0.0408, and the correlation coefficient (r2) was greater than 0.998. The LOQ and LOD were 50.0 and 20.0 ng/mL, respectively. The precision, accuracy and stability data are presented in Table 1.

3.7. Pharmacokinetic study

The plot of the mean plasma concentration versus time for CA and CA with chitosan is illustrated in Figure 7. The estimated pharmacokinetic parameters are shown in Table 2. As shown in Table 2, chitosan increased the absorption of CA during the 24 h in rats because the relative bioavailability was 174%. Compared to CA without chitosan, the C_{max} almost doubled, and the t_{max} was 180 min earlier. This indicates that the oral absorption of CA was greatly enhanced by chitosan.

The present study investigated the permeation mechanism of CA using Caco-2 cell monolayers. Based on the results of this study, paracellular passive diffusion is predominant in the A – B direction. In secretory transport, the involvement of the active transporter OATP2B1

Table 1. Within-day and between-day precision, accuracy and stability of the method for the determination of CA in rat plasma.

Conc. (ng/mL)	Within-run (n = 5)		Between-run (n = 5, three runs)		Remaining (%)
	Precision (RSD%)	Accuracy (%)	Precision (RSD%)	Accuracy (%)	
100.0	3.3	108.0	1.4	108.7	102.0
500.0	5.9	91.4	0.4	90.0	100.6
2000.0	5.4	100.3	0.4	97.2	99.4

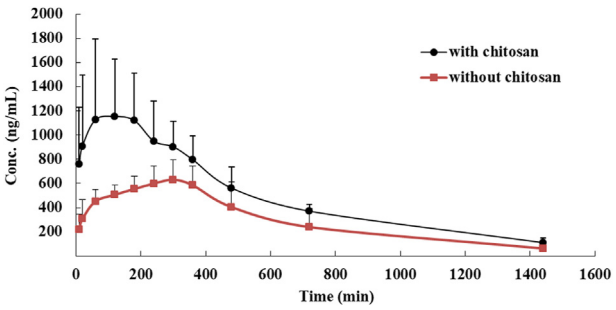

Figure 7. Mean plasma concentration-time profiles of CA in rats following intragastric (i.g., 20 mg/kg) administration of CA with or without chitosan (mean ± SD, n = 5).

Table 2. Pharmacokinetic parameters of CA with chitosan and without chitosan in rats after gavage administration.

Parameters	With chitosan	Without chitosan
C_{max} (ng/mL)	1279.3 ± 557.9*	635.8 ± 128.3
T_{max} (min)	120.0*	300.0
$t_{1/2,\lambda z}$ (min)	389.9 ± 51.5	333.0 ± 86.4
$AUC_{0\text{-}t}$ (μg·min/mL)	724.9 ± 232.5*	439.2 ± 123.
$AUC_{0\text{-}\infty}$ (μg·min/mL)	787.8 ± 248.5*	451.9 ± 136.6
CL/F (mL/min/kg)	27.9 ± 10.4	35.7 ± 23.8
$V_{d,\lambda z}$/F (mL/kg)	15612.1 ± 5507.6	16794.1 ± 12638.5
F (%)	174	

Notes: Each value represents the mean ± SD (n = 5). Significant differences were accepted at $p < 0.05$ (*).

seems to be likely, and Pgp could be in part the reason for the low transport observed from the A to B side, although an important role of the paracellular pathway has also been evidenced.

In an in vivo study, a novel UPLC method to quantify CA was developed. The validated method was illustrated to be reliable and rapid. Following oral administration, CA with chitosan showed very different pharmacokinetic profiles compared to CA without chitosan in rats. CA showed significantly higher C_{max} and AUC $_{0-\infty}$ with chitosan. This indicates that oral absorption of CA was greatly enhanced by chitosan, which could be attributed to the tight junction integrity reduction and intestinal absorption improvement. This is consistent with the results of in vitro studies.

4. Conclusions

CA was a poor absorption drug due to its low Papp value with pH-dependent. Passive paracellular transport was the main transport route of CA with minor active carrier-mediated transcellular transport. Pgp and OATP2B1 could participate in the active transport process of its transcellular pathway. Chitosan, a natural intercellular opener, could improve the absorption of CA in vitro and in vivo and could be used as a coating material for CA.

Declarations

Author contribution statement

Geng Nan Wang: Conceived and designed the experiments; Performed the experiments; Analyzed and interpreted the data; Contributed reagents, materials, analysis tools or data; Wrote the paper.

Yi Peng Li: Performed the experiments; Analyzed and interpreted the data.

Si Kun Yuan: Analyzed and interpreted the data; Contributed reagents, materials, analysis tools or data.

Hu Zhang; Juan Ren; Xin Ren: Performed the experiments.

Ju Xiang Liu: Contributed reagents, materials, analysis tools or data.

Funding statement

Geng Nan Wang was supported by National Natural Science Foundation of China [32002343], Hebei Graduate Innovation Foundation [CXZZBS2021038].

Data availability statement

Data will be made available on request.

Declaration of interests statement

The authors declare no conflict of interest.

Additional information

No additional information is available for this paper.

References

[1] P. Molgaard, S. Johnsen, P. Christensen, C. Cornett, HPLC method validated for the simultaneous analysis of cichoric acid and alkamides in *Echinacea purpurea* plants and products, J. Agric. Food Chem. 51 (2003) 6922–6933.

[2] L. Dalby-Brown, H. Barsett, A.K. Landbo, A.S. Meyer, P. Molgaard, Synergistic antioxidative effects of alkamides, caffeic acid derivatives, and polysaccharide fractions from *Echinacea purpurea* on in vitro oxidation of human low-density lipoproteins, J. Agric. Food Chem. 53 (2005) 9413–9423.

[3] J. Barnes, L.A. Anderson, S. Gibbons, D. Phillipson, *Echinacea* species (*Echinacea angustifolia* (DC.) Hell., *Echinacea pallida* (Nutt.) Nutt.,*Echinaceapurpurea* (L.) Moench): a review of their chemistry, pharmacology and clinical properties, J. Pharm. Pharmacol. 57 (2005) 304–314.

[4] M. Karsch-Völk, B. Barrett, D. Kiefer, R. Bauer, K.L.K. Ardjomand-Woelkart, *Echinacea* for preventing and treating the common cold, Cochrane Database Syt. Rev. 20 (2014) CD000530.

[5] H. Ding, X.X. Ci, H. Cheng, Q.L. Yu, D. Li, Chicoric acid alleviates lipopolysaccharide-induced acute lung injury in mice through anti-inflammatory and anti-oxidant activities, Int. Immunopharm. 66 (2019) 169–176.

[6] Y.P. Ma, W.J. Cong, H. Huang, L. Sun, A.H. Mai, K. Boonen, W. Maryam, W.D. Borggraeve, G. Luo, G. Liu, Q. Liu, L. Schoofs, F.V. Kuppeveld, J. Neyts, C. Mirabelli, W. Luyten, Identification of fukinolic acid from cimicifuga heracleifolia and its derivatives as novel antiviral compounds against enterovirus A71 infection, Int. J. Antimicrob. Agents 53 (2019) 128–136.

[7] M.G. Molinu, G. Piluzza, G. Campesi, L. Sulas, G.A. Re, Antioxidant sources from leaves of Russian Dandelion, Chem. Biodivers. 16 (2019), e1900250.

[8] M. Nazir, D. Tungmunnithum, S. Bose, S. Drouet, L. Garros, N. Giglioli-Guivac'h, B.H. Abbasi, C. Hano, Differential production of phenylpropanoid metabolites in callus cultures of *OcimumBasilicum L.* with distinct in vitro antioxidant activities and in vivo protective effects against UV stress, J. Agric. Food Chem. 67 (2019) 1847–1859.

[9] X.L. Zhu, F.H. Huang, X. Xiang, M. Fan, T.T. Chen, Evaluation of the potential of chicoric acid as a natural food antioxidant, Exp. Ther. Med. 16 (2018) 3651–3657.

[10] J. Langland, B. Jacobs, C.E. Wagner, G. Ruiz, T.M. Cahill, Antiviral activity of metal chelates of caffeic acid and similar compounds towards herpes simplex, VSV-Ebola pseudotyped and vaccinia viruses, Antivir. Res. 160 (2018) 143–150.

[11] S.A. Petropoulos, Â. Fernandes, L. Barros, I.C. Ferreira, A comparison of the phenolic profile and antioxidant activity of different Cichorium Spinosum L. ecotypes, J. Sci. Food Agric. 98 (2018) 183–189.

[12] Y. Wang, Z.J. Lin, B. Zhang, Z.X. Jiang, F.F. Guo, T. Yang, L. Cichoriumintybus, Extract suppresses experimental gout by inhibiting the NF-κB and NLRP3 signaling pathways, Int. J. Mol. Sci. 20 (2019) 4921–4935.

[13] B. SarathKumar, B.S. Lakshmi, Silico investigations on the binding efficacy and allosteric mechanism of six different natural product compounds towards PTP1B inhibition through docking and molecular dynamics simulations, J. Mol. Model. 25 (2019) 272–288.

[14] G.N. Wang, J.P. Wang, H. Zhang, Y.T. Miao, Y. Bai, J.X. Liu, Determination of chicoric acid content in plasma and urine of rats by ultra-performance liquid chromatography and related pharmacokinetic study, Chin. J. Vet. Med. 57 (2021) 97–101.

[15] D. Dimitrijevic, A. Shaw, A.T. Florence, Effects of some non-ionic surfactants on transepithelial permeability in Caco-2 cells, J. Pharm. Pharmacol. 52 (2000) 157–162.

[16] B.J. Aungst, Intestinal permeation enhancers, J. Pharmacol. Sci. 89 (2000) 429–442.

[17] T. Okuda, K. Kadotsuji, C. Takayama, K. Hanada, F. Mukaizawa, K.I. Ogawara, K. Higaki, T. Kimura, Involvement of intra-cellular Ca^{2+} dynamics in cytoprotective

action by amino acids and cytotoxicity by sodium laurate, an absorption enhancer, J. Pharmacol. Sci. 95 (2006) 2256–2265.
[18] G.S. Gordon, A.C. Moses, R.D. Silver, J.S. Flier, M.C. Carey, Nasal absorption of insulin: enhancement by hydrophobic bile salts, Proc. Natl. Acad. Sci. U.S.A. 82 (1985) 7419–7423.
[19] E.A.E.-H. Mohamed, T.E.-S. Mohamed, E.S. Manal, M.Z. Nidal, A. Muhammad, E.B. Gaber, F.K. Asmaa, M.A.E.-H. Yasmina, A.A.-S. Adham, Antimicrobial and antioxidant properties of chitosan and its derivatives and their applications: a review, Int. J. Biol. Macromol. 164 (2020) 2726–2744.
[20] N. Taskeen, I. Muhammad, M. Alan, Improving carvacrol bioaccessibility using core-shell carrier-systems under simulated gastrointestinal digestion, Food Chem. 353 (2021), 129505.
[21] C.D.S. Natalia, T.D.B.-A. Tais, B.G.A. Odílio, Milena Martelli-Tosi, Extraction of phenolic compounds from acerola by-products using chitosan solution, encapsulation and application in extending the shelf-life of guava, Food Chem. 354 (2021), 129553.
[22] R. Parthiban, S. Swadeshmukul, Hydrothermally treated chitosan hydrogel loaded with copper and zinc particles as a potential micronutrient-based antimicrobial feed additive, Front. Vet. Sci. 2 (2015) 62–70.
[23] J.M. Smith, M. Dornish, E.J. Wood, Involvement of protein kinase C in chitosan glutamate-mediated tight junction disruption, Biomaterials 26 (2005) 3269–3276.
[24] K. Sonaje, Y.J. Chen, H.L. Chen, S.P. Wey, J.H. Juang, H.N. Nguyen, C.W. Hsu, K.J. Lin, H.W. Sung, Entericcoated capsules filled with freeze-dried chitosan/poly(gamma-glutamic acid) nanoparticles for oral insulin delivery, Biomaterials 31 (2010) 3384–3394.
[25] T.-H. Yeh, L.W. Hsu, M.T. Tseng, P.L. Lee, K. Sonjae, Y.C. Ho, H.W. Sung, Mechanism and consequence of chitosan-mediated reversible epithelial tight junction opening, Biomaterials 32 (2011) 6164–6173.
[26] J. Kinzi, M. Grube, H.E.M. Schwabedissen, OATP2B1 – the underrated member of the organic anion transporting polypeptide family of drug transporters? Biochem. Pharmacol. 188 (2021) 114534–114548.
[27] A. Kosińska-Cagnazzo, S. Diering, D. Prim, W. Andlauer, Identification of bioaccessible and uptaken phenolic compounds from strawberry fruits in in vitro digestion/Caco-2 absorption model, Food Chem. 170 (2015) 288–294.
[28] C. Chen, T. Li, Z.X. Chen, L. Wang, X.H. Luo, Absorption rates and mechanisms of avenanthramides in a caco-2 cell model and their antioxidant activity during absorption, J. Agric. Food Chem. 68 (2020) 2347–2356.
[29] M.J. Zamek-Gliszczynski, M.E. Taub, P.P. Chothe, X.Y. Chu, K.M. Giacomini, R.B. Kim, A.S. Ray, S.L. Stocker, J.D. Unadkat, M.B. Wittwer, C. Xia, S.W. Yee, L. Zhang, Y. Zhang, International Transporter Consortium International Transporter Consortium (2018) Transporters in drug development: 2018 ITC recommendations for transporters of emerging clinical importance, Clin. Pharmacol. Ther. 104 (2018) 890–899.
[30] M.Q. Chen, S.Y. Hu, Y. Li, A.A. Gibson, Q. Fu, S.D. Baker, A. Sparreboom, Role of Oatp2b1 in drug absorption and drug-drug interactions, Drug Metab. Dispos. 48 (2020) 419–425.
[31] Y. Chen, X.M. Liu, R.L. Pan, X.X. Zhu, A. Steinmetz, Y.H. Liao, N. Wang, B. Peng, Q. Chang, Intestinal transport of 3,6'-disinapoylsucrose, a major active component of Polygala tenuifolia, using Caco-2 cell monolayer and in situ rat intestinal perfusion models, Planta Med. 79 (2013) 1434–1439.
[32] J.W. Polli, S.A. Wring, J.E. Humphreys, L. Huang, J.B. Morgan, L.O. Webster, C.S. Serabjit-Singh, Rational use of in vitro P-glycoprotein assays in drug discovery, J. Pharmacol. Exp. Therapeut. 299 (2001) 620–628.
[33] F. Xu, J. Zheng, F.S.G. Cheung, T. Chan, L. Zhu, H.X. Zhu Ge, F.F. Zhou, The inhibitory effects of the bioactive components isolated from scutellaria baicalensis on the cellular uptake mediated by the essential solute carrier transporters, J. Pharmacol. Sci. 102 (2013) 4205–4211.
[34] S. Yee, Vitro permeability across Caco-2 cells (colonic) can predict in vivo (small intestinal) absorption in man–fact or myth, Pharm. Res. (N. Y.) 14 (1997) 763–766.
[35] I. Hubatsch, E.G.E. Ragnarsson, P. Artursson, Determination of drug permeability and prediction of drug absorption in Caco-2 monolayers, Nat. Protoc. 2 (2007) 2111–2119.
[36] Q. Yu, Z. Wang, P. Li, Q. Yang, The effect of various absorption enhancers on tight junction in the human intestinal Caco-2 cell line, Drug Dev. Ind. Pharm. 39 (2013) 587–592.
[37] S. Pichardo, V. Devesa, M. Puerto, D. Vélez, A.M. Cameán, Intestinal transport of Cylindrospermopsin using the Caco-2 cell line, Toxicol. Vitro 38 (2017) 142–149.
[38] K. Sugano, M. Kansy, P. Artursson, A. Avdeef, S. Bendels, L. Di, G.F. Ecker, B. Faller, H. Fischer, G. Gerebtzoff, H. Lennernaes, F. Senner, Coexistence of passive and carrier-mediated processes in drug transport, Nat. Rev. Drug Discov. 9 (2010) 597–614.
[39] P. Anilkumar, A.V. Badarinath, N. Naveen, K. Prasad, B. Ravi Shankar Reddy, M. Hyndhavi, A rationalized description on study of intestinal barrier, drug permeability and permeation enhancers, J. Global Trends Pharmaceut. Sci. 4 (2011) 431–449.
[40] S.T. Ballard, J.H. Hunter, A.E. Taylor, Regulation of tight-junction permeability during nutrient absorption across the intestinal epithelium, Annu. Rev. Nutr. 15 (1995) 35–55.
[41] S. Leuthold, B. Hagenbuch, N. Mohebbi, C.A. Wagner, P.J. Meier, B. Stieger, Mechanisms of pH-gradient driven transport mediated by organic anion polypeptide transporters, Am. J. Physiol. Cell Physiol. 296 (2009) C570–582.
[42] T. Morita, T. Akiyoshi, R. Sato, K. Katayama, K. Yajima, H. Kataoka, A. Imaoka, Y. Sugimoto, H. Ohtani, pH-dependent transport kinetics of the human organic anion-transporting polypeptide 1A2, Drug Metabol. Pharmacokinet. 35 (2020) 220–227.
[43] T. Nozawa, K. Imai, J. Nezu, A. Tsuji, I. Tamai, Functional characterization of pH sensitive organic anion transporting polypeptide OATP-B in human, J. Pharmacol. Exp. Ther. 308 (2004) 438–445.
[44] M.L. Lucas, B.T. Cooper, F.H. Lei, I.T. Johnson, G.K. Holmes, J.A. Blair, W.T. Cooke, Acid microclimate in coeliac and Crohn's disease: a model for folate malabsorption, Gut 19 (1978) 735–742.
[45] M. Keiser, L. Kaltheuner, C. Wildberg, J. Müller, M. Grube, C.D. Partecke Li, Heidecke, S. Oswald, The organic anion-transporting peptide 2B1 is localized in the basolateral membrane of the human jejunum and caco-2 monolayers, J. Pharmacol. Sci. 106 (2017) 2657–2663.